Single-Step Synthesis to Control the Photoluminescence Quantum Yield and Size Dispersion of CdSe Nanocrystals

Celso de Mello Donegá,* Stephen G. Hickey, Sander F. Wuister, Daniel Vanmaekelbergh, and Andries Meijerink

Debye Institute, Chemistry of Condensed Matter, Utrecht University, PO Box 80000, 3508TA Utrecht, The Netherlands

Received: October 8, 2002

A comprehensive investigation is presented on the factors governing the photoluminescence (PL) quantum yields (QYs) and size dispersion of colloidal CdSe nanocrystals. The temporal evolution of the ensemble PL properties (absorption and luminescence spectra, QYs and lifetimes) during growth at different temperatures (170−310 °C) and different Cd:Se ratios was followed for several hours (2−6 h). The QY values increase during the growth to a maximum and, after a variable time interval (from minutes to hours, depending on the growth temperature), decrease gradually. Low QYs are due to poor passivation, surface disorder, and surface degradation, which arise at different stages of the growth. High QYs can be achieved and maintained only under an ideal combination of growth temperature, solvent composition, and Cd:Se ratio, which leads to an optimum surface. The overgrowth of a fresh surface layer restores high QYs to CdSe nanocrystals with decreased efficiencies because of surface degradation. The insight gained in this investigation enabled us to achieve a high degree of reproducibility and control over the emission color (green to red), bandwidth (90 meV), lifetimes (30 ns), and quantum yields (50−85%) of colloidal CdSe nanocrystals without any postpreparative treatment.

Introduction

Nanocrystalline semiconductors have attracted great interest over the past years because their properties are remarkably different from bulk semiconductors and can be tailored by a judicious control of particle composition, size, and surface.[1−6] These characteristics arise from several phenomena (viz. quantum confinement of charge carriers, surface effects, and geometrical confinement of phonons)[1−6] and have turned semiconductor nanocrystals into promising materials for many applications, such as light-emitting diodes,[7−10] lasers,[11,12] holographic optical memories,[13] photonic band-gap crystals,[14] ultrafast photonic switches,[2] and biomedical tags for fluoroimmunoassays, nanosensors, and biological imaging.[15−20]

To realize this wide range of potential applications the luminescent properties (i.e., emission color, quantum yield, luminescence lifetime, and stability) of semiconductor nanocrystals must be strictly controlled. The development of a number of colloidal synthetic routes over the last years, particularly for CdSe,[21−35] has yielded a remarkable degree of control over the size[24−33] and shape[26,30,32] of the nanocrystals. Although rather high photoluminescence (PL) quantum yields (≥40%) have been obtained by inorganic[23−25,29,31,35−38] or organic[28,29,33,35] capping of colloidal CdSe nanocrystals, the control and reproducibility of the PL quantum yields has remained an elusive issue. The core/shell CdSe/ZnS nanocrystals illustrate very well this difficulty with reported quantum yields ranging from 10% to 60%,[23,25,29,31,35−38] although this is widely recognized as a successful passivation method. Despite this, only recently some of the factors determining the PL efficiency of nanocrystals have been properly addressed.[33−35]

The influence of the initial ratio between the Cd and the Se precursors on the temporal evolution of the ensemble PL quantum yield of CdSe nanocrystals during their growth at 290 °C in a coordinating solvent (TOPO:HDA:TBP:DOA; where TOPO= trioctylphosphine oxide; HDA= hexadecylamine; TBP= tributylphosphine; DOA= dioctylamine) has been investigated by Qu and Peng.[33] The PL quantum yield was observed to increase monotonically during growth to a maximum value (dubbed the "bright point"[33]) and then gradually decrease. The position and temporal width of the "bright point", the highest quantum yield, the growth kinetics, and the sharpness of the PL peak were all reported to be strongly dependent on the initial Cd:Se ratio (from 2:1 to 1:10).[33] The existence of the "bright point" was interpreted as a signature of an optimal surface structure/reconstruction of the nanocrystals grown under a given set of initial conditions.

Talapin et al.[34] investigated the distribution of properties within ensembles of colloidally grown II−VI (CdSe and CdTe) and III−V (InAs) semiconductor nanocrystals, by analyzing size-selected fractions. The CdSe and InAs colloids were organometallically prepared by injection into a hot coordinating solvent (TOPO:TOP; growth temperatures: 300 °C and 260 °C; TOP = Trioctylphosphine), whereas CdTe nanocrystals were synthesized in an aqueous medium at 100 °C. An excess of the metal cation precursor (Cd or In) was used in all three cases. A drastic difference was observed between the PL efficiencies of fractions size-selected from the same ensemble and was attributed to differences in surface disorder of the nanocrystals as a consequence of the Ostwald ripening growth mechanism.[34] The particles with the lowest growth rate within the ensemble were assumed to have the lowest degree of surface disorder and therefore the highest PL quantum yield at any given reaction conditions.[34]

* To whom correspondence should be addressed. Phone: +31-30-2532226. Fax: +31-30-2532403. E-mail: C.deMelloDonega@phys.uu.nl.

10.1021/jp027160c CCC: $25.00
Published on Web 12/12/2002

A large difference between the PL quantum yields of individual CdSe nanocrystals within an ensemble has also been reported by Ebenstein et al.[35] based on the investigation of CdSe/ZnS core/shell nanoparticles (ensemble quantum yields ranging from 12% to 48%) by correlated atomic force and fluorescence microscopy. The results revealed the presence of a significant portion of dark particles (ca. 50−70% of the ensemble) in all samples.[35] Samples with a higher ensemble QY were shown to have a larger fraction of bright particles, accompanied by an increased single-particle QY (from 37% to 94%). The sources for this inhomogeneity, however, were not discussed.

Although the works reviewed above[33−35] have contributed to a better understanding of some of the parameters controlling the photoluminescence quantum yield of colloidal semiconductor nanocrystals, there are still many unanswered questions. The crucial role of the surface is clearly demonstrated by both Qu and Peng[33] and Talapin et al.,[34] but the mechanisms underlying the correlation between the surface quality and the growth conditions have yet to be determined. For example, the role of the growth temperature was not addressed in both works. Most importantly, a comprehensive investigation of several parameters (viz. temperature and Cd/Se precursor ratio) in a single synthetic system is still lacking. In this paper, we report on the temporal evolution of the ensemble band-edge luminescence quantum yield for CdSe nanocrystals grown at different temperatures and under different Cd:Se precursor ratios. The investigations are carried out in one of the most successful coordinating solvents so far reported (viz. TOPO:HDA:TOP[29]) in order to make the roles of the growth temperature and precursor ratio more evident. In addition to determining the PL quantum yields, the band-edge luminescence full-width at half-maximum, and the particle sizes, we have performed room temperature decay time measurements for the band-edge luminescence. It is well established in the literature that the exciton decay dynamics are strongly dependent on the surface properties of semiconductor nanocrystals,[4−6,23,25,38−42] although the details of this dependence and the nature of the emitting state are not yet fully understood. To the best of our knowledge, this is the most comprehensive investigation to date on the factors controlling the quantum yield of the band edge photoluminescence for colloidal CdSe nanocrystals.

Experimental Section

Chemicals. Trioctylphosphine (TOP, tech. grade 90%), trioctylphosphine oxide (TOPO, 99%), hexadecylamine (HDA, 90%), anhydrous triethylorthoformate (TEOF, 98%), and water free toluene were all purchased from Aldrich. Selenium powder 200 mesh (99.99%) and dimethylcadmium (99.99%) were purchased from Chempur and ARC Technologies, respectively. All reagents were used as received with the exception of TOPO and HDA. Before use, both of these reagents were dried and degassed by heating under vacuum, TOPO at 200 °C for 4 h and HDA at 180 °C for 6 h.

Synthesis. Colloidal solutions of CdSe nanocrystals were prepared by a modified version of the high-temperature organometallic synthesis developed by Talapin et al.[29] The main modifications are a larger reaction volume, the addition of a dehydrating agent (viz. TEOF[43]) to ensure the removal of any residual moisture present in the coordinating solvent, variable growth temperatures, and different Cd:Se precursor ratios. The use of TEOF was found to be necessary in order to achieve the high degree of reproducibility reported in this paper for the growth kinetics and the QYs. The coordinating solvent composition (67 wt %TOPO: 33 wt %HDA) was the same as that reported by Talapin et al.[29] to be the most adequate in achieving a slow growth and minimizing Ostwald ripening. In addition, the TOPO:HDA mixture has been shown to yield higher quantum yields than TOPO alone.[28,29,33] High precursor concentrations were used, because this has been demonstrated, both experimentally and theoretically,[29,44,45] to be important in achieving fast size focusing and slow defocusing. Following Talapin et al.[34,45] and Peng et al.,[32,33,44] we use the term "ensemble" to describe the whole population of particles present in the colloidal solution at a given time and the term "monomer" indicates any species, other than nanocrystals, containing Cd or Se which are necessary for the formation and growth of nanocrystals after the hot-injection. The term "precursor" is used to indicate the species containing Cd or Se prior to the hot-injection.

The synthesis was carried out in a glovebox under Argon employing standard oxygen and moisture free conditions (less than 5 ppm O_2 and H_2O). A total of 20 g of TOPO, 10 g of HDA, and 2 mL of TEOF were placed into a 250 mL three-neck, round-bottom flask and heated slowly to 330 °C. At this point, the heating mantle was removed, and the temperature was allowed to fall. When the temperature had reached 300 °C, 10 mL of the TOP/selenium/dimethylcadmium solution, containing a Cd:Se molar ratio of either 2:1, 1:1, or 1:5, was quickly injected into the mixture using a syringe. After the injection, the temperature was allowed to fall further to ∼150 °C, which is below the reported growth temperature.[21,29] The reaction mixture was then stabilized at the desired growth temperature (170−280 °C). Small volume aliquots (∼0.1 mL) were taken at regular time intervals after the point of injection and placed into 5 mL of anhydrous toluene. The resulting samples were further diluted with anhydrous toluene for subsequent characterization. No further postpreparative procedure was employed after sampling, except for the samples to be investigated by transmission electron microscopy, which were treated by precipitation with anhydrous methanol followed by redissolution in anhydrous toluene. The samples for optical characterization were sealed in vials under argon before being removed from the glovebox, thus preventing any contact with air.

Characterization. All optical measurements were carried out promptly (within 12 h after the synthesis, unless otherwise stated) on samples with a low optical density (≤0.1 at the emission maximum, 0.2−0.4 at 400 nm) in order to minimize reabsorption and avoid absorption saturation. Lifetime measurements were performed on samples which remained under argon inside the sealed vials. A Pico Quant PDL 800-B laser was used as the excitation source (λ_{exc}= 406 nm, 55 ps pulse width, 2.5 MHz repetition rate). The luminescence was filtered through a 410 nm cutoff filter, dispersed by a 0.1 m monochromator (1350 lines/mm grating, blazed at 500 nm) and detected by a Hamamatsu photomultiplier tube (H5738P-01). Luminescence decay curves were obtained by pulse height analysis using a Time Harp 100 multichannel computer card. The acquisition time for a full time trace was typically shorter than 10 s.

Photoluminescence spectra were acquired upon excitation at 400 nm, using a 450 W Xe lamp as the excitation source and a double grating 0.22 m SPEX monochromator. The emitted light was collected at 90° from the excitation beam and collimated into an optical fiber cable leading to a 0.3 m monochromator (Acton Pro SP-300i, 150 lines/mm grating, blazed at 500 nm). An optical cutoff filter was used to remove residual excitation light. The dispersed luminescence light was detected by a liquid-nitrogen-cooled Princeton Instruments CCD

camera (1024 × 256 pixels). The measurements were performed on samples in open quartz cuvettes immediately after opening the sealed vials. To avoid photocuring[34,46] and/or photoetching,[36,47] short acquisition times (≤4 s) were used. UV−visible absorption spectra were recorded on a Perkin-Elmer Lambda 16 UV/vis spectrophotometer. The excitonic transition energy, derived from the maximum of the first exciton absorption peak, was used to estimate the average nanocrystal diameter by fitting to a function calibrated to experimental data available in the literature.[21,22,27]

The mean particle sizes for some samples of CdSe nanocrystals were also determined by transmission electron microscopy (FEI TECNAI G^2 T20F-200 keV), and found to be in good agreement (i.e., ±10%) with the values estimated from the exciton absorption peaks. Sample preparation for the TEM and HRTEM measurements was done by placing a drop of the colloidal suspension onto a carbon/pioloform film supported on Cu grids and allowing it to dry under air at room temperature. Considering the aim of this work, UV−visible absorption spectroscopy is a more convenient technique to estimate the mean diameters of CdSe nanocrystals in colloidal suspensions, because it has the important advantages of probing the whole ensemble used for the quantum yield and lifetime measurements and allowing the analysis of the crude samples (as-prepared and after the measurements).

Photoluminescence quantum yields (QY) were obtained by comparison with a standard (Rhodamine B in ethanol) and using data derived from the luminescence and the absorption spectra, as follows:

$$\mathrm{QY} = \left(\frac{1 - T_{\mathrm{ST}}}{1 - T_{\mathrm{X}}}\right)\left(\frac{\Delta\Phi_{\mathrm{X}}}{\Delta\Phi_{\mathrm{ST}}}\right)q_{\mathrm{ST}}$$

where T_{ST} and T_X are the transmittances at 400 nm for the standard and the sample, respectively, and q_{ST} is the quantum yield of the standard (90%, as indicated by the supplier, Exciton). The terms $\Delta\Phi_X$ and $\Delta\Phi_{ST}$ give the integrated emitted photon flux (photons s^{-1}) for the sample and the standard respectively, upon 400 nm excitation. Utmost care was taken to ensure a constant and reproducible position for the sample/standard holder and unchanged instrumental conditions throughout the measurements. The values of $\Delta\Phi_X$ and $\Delta\Phi_{ST}$ are determined from the photoluminescence spectra corrected for the instrumental response, by integrating the emission intensity over the desired spectral range. Only the band-edge luminescence peak was integrated (any other luminescence bands, such as defect associated luminescence or solvent fluorescence, were discarded as background). Correction for luminescence reabsorption was performed, based on the Lambert−Beer law, but was found to be unnecessary for optical densities ≤0.1. The accuracy of the method is estimated to be ±10%, based on duplicate measurements.

Results

Influence of the Growth Temperature. To be able to distinguish between CdSe quantum dot luminescence and background emission, first the luminescence properties of the coordinating solvent mixture (TOPO:HDA) without Cd/Se addition was investigated. Prior to heating, no emission could be detected. However, after heating to temperatures above ~300 °C, the solvent mixture shows a broad band luminescence in the blue upon excitation in the UV region (Figure 1). This blue luminescence exhibits a quantum yield of 8 ± 2% and a strongly nonexponential decay ($\tau \sim 4$ ns) and is ascribed to an

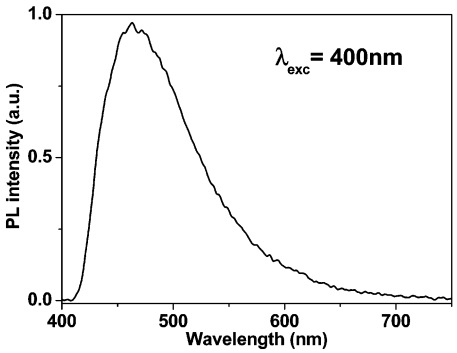

Figure 1. Room-temperature photoluminescence spectrum (λ_{exc}= 400 nm) of the coordinating solvent mixture (TOPO:HDA) after heating to 330 °C, diluted in toluene.

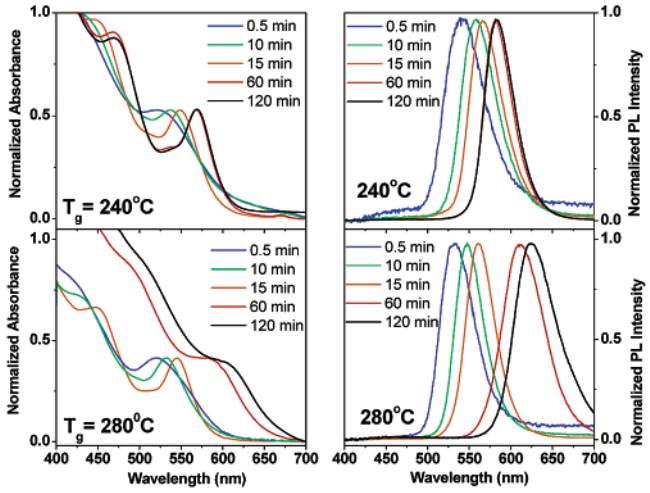

Figure 2. Temporal evolution of the absorption (left panels) and photoluminescence (right panels) spectra of crude solutions of colloidal CdSe nanocrystals during their growth at 240 (top panels) and 280 °C (bottom panels). The monomer concentration and the Cd:Se precursor ratio (1:5) are the same in both growth temperatures.

undetermined organic substance, which develops in the mixture upon heating. The amount of this substance is very small, as judged from its absorption, and varies from synthesis to synthesis, depending on the duration of the heating above 300 °C. For samples of colloidal CdSe nanocrystals with low QYs (<10%), it is necessary to correct for the coordinating solvent luminescence and competitive absorption. For samples with higher QYs, this correction was found to be unnecessary.

Figure 2 presents the temporal evolution of the absorption and luminescence spectra of crude samples of colloidal CdSe nanocrystals grown at two different temperatures (240 and 280 °C). The intensities have been normalized to the maximum of the first exciton peak (absorption or band-edge photoluminescence). The CdSe concentration (67 mmol/Kg solvent) and the Cd:Se precursor ratio (1:5) are the same in both cases. The Cd:Se ratio was chosen based on the results recently reported by Qu and Peng,[33] which showed that, under the conditions employed in the investigation, a 1:5 Cd:Se ratio leads to the highest quantum yields.

The growth of the particles is clearly evidenced in Figure 2 by the shift of both absorption and emission spectra to longer wavelengths. The relative intensities of the defect-associated luminescence (a broad band with maximum at ~700 nm, usually referred to as "deep-trap emission"[21−23,39]) and of the coordinating solvent fluorescence (Figure 1 above) are weak, even for the initial samples, and decrease in time as a result of the increase of the band edge luminescence quantum yield. The

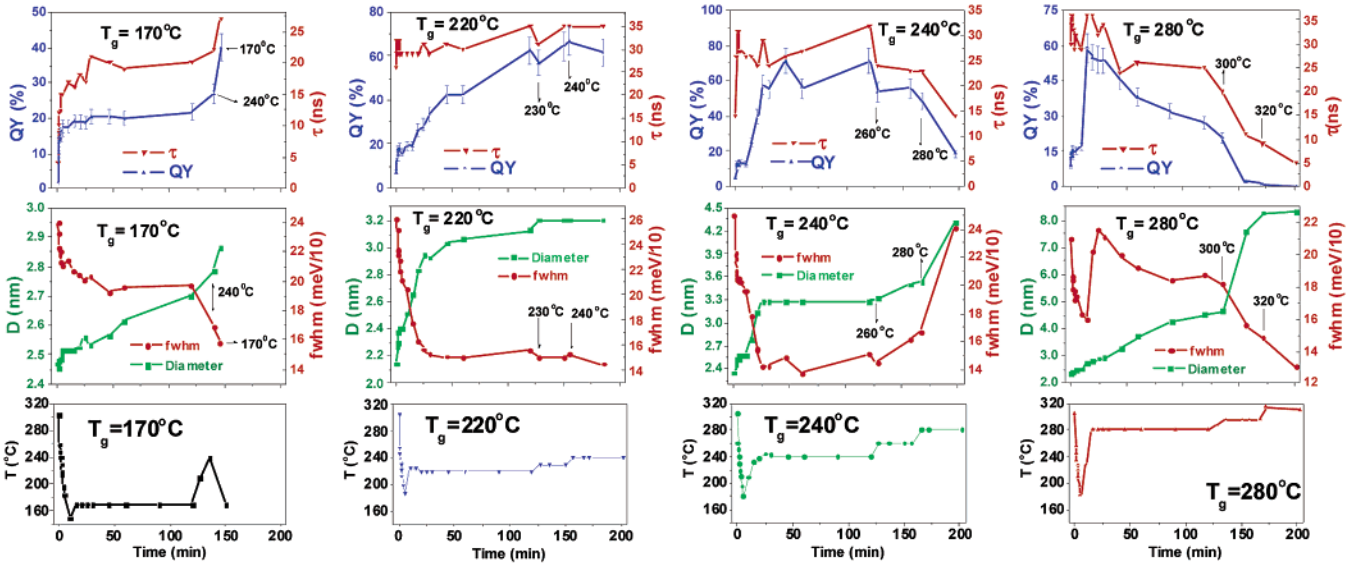

Figure 3. Temporal evolution of the band-edge photoluminescence quantum yields (QY, blue up triangles), lifetimes (τ, red down triangles), fwhm (red circles), and particle sizes (D, green squares) of crude solutions of colloidal CdSe nanocrystals during their growth at four different temperatures (170, 220, 240, and 280 °C, from left to right). The temperature trends in each synthesis are also presented (bottom panels). The CdSe concentration (67 mmol/Kg solvent) and the Cd:Se precursor ratio (1:5) are the same in all cases. Trend lines are added for each plot to guide the eyes.

widths of the exciton absorption and of the band-edge luminescence peaks reflect the ensemble size polydispersity. A substantial difference in the growth evolution is observed between the two growth temperatures. The temperature dependence was investigated systematically for four different growth temperatures (170, 220, 240, and 280 °C). The temperature trend for each synthesis is shown in Figure 3. The initial cooling after the injection is the same in all cases. Each series consists of a period of growth at constant temperature (170, 220, 240, or 280 °C) followed by an increase to two subsequent temperature values, except in the case of the 170 °C synthesis, in which the temperature was raised to 240 °C for only a brief time interval (~1 min) and then brought back to 170 °C.

The temperature dependence of the temporal evolution of some selected ensemble properties (viz. particle sizes, quantum yields, lifetimes, and full-width at half-maximum for the band-edge luminescence) is summarized in Figure 3 for crude colloidal CdSe nanocrystals grown at different temperatures. The Cd:Se ratio (1:5) and the concentration of both Cd and Se precursors (67 and 335 mmol/Kg solvent, respectively) are the same in all cases.

The decay curves of the band-edge photoluminescence provide important information on the recombination of photoinduced charge carriers in CdSe nanocrystals. Nevertheless, the lifetimes presented in Figure 3 can convey only part of this information. To illustrate this, Figure 4 shows the decay curves of some selected samples grown at 240 °C (0.5; 20 and 120 min of growth), measured 12 and 36 h after preparation. The decay curves are nonexponential. As the growth proceeds, the nonexponential character decreases, and the exponential tail observed for the most efficient quantum dots reflects the lifetime of the exciton emission due to radiative recombination. The analysis of the decay curves of the emission from samples taken at early stages during growth is complicated. The nonexponential decay curves have been analyzed by multiexponential[38,41,42,48] or stretched exponential[35,48] fittings. The nonexponential character is due to a large distribution of luminescence lifetimes for different particles because of different rates for nonradiative processes in individual particles depending on the defect structure. Rather than trying to fit the decay curves to a certain

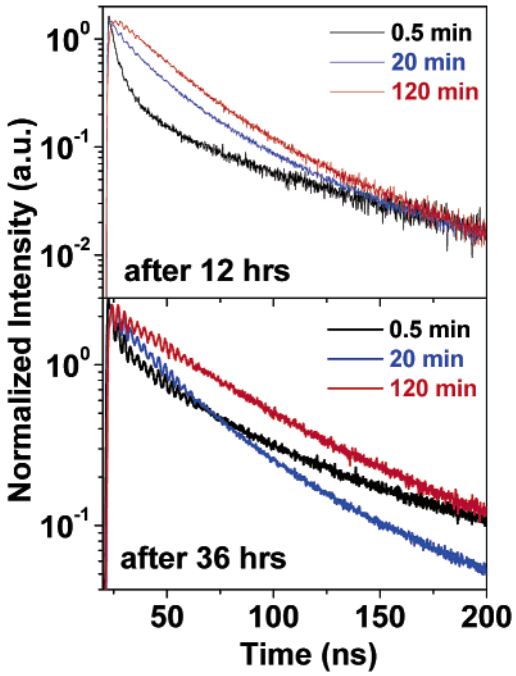

Figure 4. Representative examples of the band-edge photoluminescence decay curves of crude solutions of colloidal CdSe nanocrystals grown at 240 °C (Cd:Se = 1:5), measured 12 (top panel) and 36 h (bottom panel) after preparation (λ_{exc} = 406 nm).

model, we use the time at 1/e of the initial intensity as an estimate of the lifetime, because it allows for a better comparison between samples than using models with various fitting parameters. An interesting observation is that for samples taken at early stages of growth (less than 20 min of reaction time) the luminescence decay curve changes significantly over time at room temperature, indicating that structural relaxation of the CdSe nanocrystals occurs. The long exponential tail ($\tau \sim 100$ ns) observed in the decay curves of the samples with quantum yields below ~20% (see, e.g., Figure 4, 0.5 min) is longer than the exciton emission lifetime and is probably related to radiative recombination at defects. It is important to notice that the

photoluminescence decay measurements and the lifetimes derived from them will be biased toward the brightest nanocrystals within the ensemble, because the species emitting more photons will give a larger contribution to the detected signal. This fact may be advantageously employed to provide further information on the distribution of properties within the ensemble, when combined with statistically unbiased averaged properties such as ensemble quantum yields.

The correlation between the growth and the luminescence properties, and the strong influence of the growth temperature, are evident in Figure 3. The full width at half-maximum of the band-edge luminescence peak will reflect the size distributions of the CdSe nanocrystals, thus being a good indicator of size focusing or defocusing. We did not observe a significant difference between the widths derived from the exciton absorption or PL bands. Therefore, we are presenting here the fwhm's derived from the PL peaks, because they are more accurate. The trends for the lifetimes follow very closely those of the quantum yields, except for the initial samples (up to 15−30 min of reaction time) grown at 220, 240, and 280 °C, which will be discussed later.

At 170 °C, both the QY and the lifetimes undergo a rapid increase in the initial 10 min after the injection but stabilize at rather low values after ∼30 min (20% and ∼20 ns, respectively), changing only when the temperature is raised to 240 °C after 120 min. Simultaneously, growth accompanied by focusing is observed. After 50 min, the size focusing stops, albeit the growth proceeds. The brief temperature increase to 240 °C has a pronounced effect: the growth and size focusing accelerate, with a simultaneous increase of both the QY and the lifetime. As it will become clear below, the growth behavior at 170 °C is rather unique in this respect. The growth and the focusing are faster at 220 °C than at 170 °C. Focusing stops after ∼30 min, stabilizing in a narrower size distribution than that achieved at 170 °C, whereas growth proceeds, although at a slower rate than in the initial period. The QY increases continuously, whereas the lifetimes are essentially constant (∼30 ns) throughout the growth. After 120 min, both the growth and the QY appear to approach a plateau. Raising the temperature to 230 °C slightly decreases the QY and the lifetime, which however quickly recover. The final QY, lifetime, and size are the same as observed after ∼60 min of growth at 240 °C.

The CdSe nanocrystals grow quickly at 240 °C, with a pronounced focusing, and both the size and the size polydispersity stabilize ∼30 min after the injection. Concomitantly, the QY increases monotonically and reaches a maximum ∼20 min after the stationary size regime was achieved. The size, polydispersity, QY, and lifetime remain essentially constant until the temperature is raised to 260 °C, which leads to growth with size defocusing and decreases both the QY and the lifetime. Raising the temperature to 280 °C results in an even more pronounced decrease in QY and lifetime and increase in the growth and size defocusing rates. The QY rapidly reaches a maximum for growth at 280 °C; however, it starts to decrease very shortly afterward. Higher temperatures make the QY and lifetime drop even faster, until the ensemble of CdSe nanocrystals is essentially nonluminescent. Simultaneously, growth accompanied by focusing proceeds, becoming increasingly faster as the temperature is increased further.

The results described above reveal a clear and yet complex dependence between the ensemble quantum yields of CdSe nanocrystals and their growth temperature. This dependence implies that there is an ideal growth temperature in the system presently investigated. A zero-growth regime seems to be important to achieve high quantum yields (>50%) at growth temperatures equal to or higher than 240 °C. However, at temperatures below 240 °C, the behavior is clearly the opposite: an increase in temperature improves the quantum yields, even though the ensemble growth rates become larger. Among the temperatures investigated here, 240 °C is the best growth temperature and will thus be used to further investigate the influence of the Cd:Se ratio on the luminescent properties of CdSe nanocrystals.

Influence of the Cd:Se Precursor Ratio. The influence of the initial Cd:Se precursor molar ratio, while keeping the growth temperature constant at 240 °C, was investigated for three different values (viz. 2:1; 1:1, and 1:5), chosen to cover the limits from a large excess of Cd precursor to a large excess of Se precursor. The CdSe concentrations for the syntheses with the 1:1 and 1:5 ratios were the same (viz. 67 mmol/Kg solvent). For the 2:1 ratio, a lower concentration was used because our experiments indicate that only a limited amount of Cd monomer is stable under the conditions prevalent during the synthesis. Concentrations exceeding this limit lead to precipitation of metallic Cd and uncontrolled growth of large (>20 nm) CdSe crystals, as evidenced by transmission electron microscopy, EDX (energy-dispersive X-ray analysis), and X-ray diffraction analysis. We note that the precipitation of metallic cadmium after injection of $Cd(CH_3)_2$ in hot TOPO under strictly water and oxygen-free conditions has also been observed by other groups.[49] The best compromise between a CdSe concentration as close as possible to those used in the other experiments and a significant Cd precursor excess was achieved for a 2:1 Cd:Se ratio and a CdSe concentration equal to 37 mmol/Kg solvent.

The temporal evolution of the particle sizes and the quantum yields, lifetimes, and full-width at half-maximum (fwhm) for the band-edge luminescence for ensemble crude samples of colloidal CdSe nanocrystals was followed for each Cd:Se ratio. The results are presented in Figure 5. A zero-growth regime is achieved for all three ratios but after different growth durations. Nevertheless, the final size is essentially the same in all three cases: ∼3.5 nm. The particles grow with size focusing and the polydispersity stabilizes in a minimum when the growth stops. It can be observed that growth under an excess of Se monomer leads to the slowest growth rate and the smallest size polydispersity. For the 2:1 Cd:Se ratio synthesis, an extra TOP−Se solution was slowly added after 120 min of growth, so that after the addition the Cd:Se ratio was 1:5. The nanocrystals grow after the addition, whereas the size polydispersity of the ensemble does not noticeably increase, indicating that the extra Se promotes the growth of preexisting particles, rather than leading to a new nucleation event. An extra Cd:Se solution, corresponding to 50% of the initially injected amount, was slowly added to the 1:5 ratio synthesis after 230 min growth. As expected, the extra addition induces growth of the preexisting CdSe nanocrystals, without promoting size defocusing.

The narrowest observed fwhm (90 meV; Figure 5, 1:5 synthesis) implies a monodisperse ensemble (size dispersion ≤5%[29,32]), comparable with samples after several stages of size-selective precipitation,[21,25,44] even though no postpreparative treatment was applied in the present case. The narrow size distribution of the crude ensembles of colloidal CdSe nanocrystals synthesized in this work is also evidenced by TEM. A representative example is presented in Figure 6, for a sample of CdSe nanocrystals grown at 240 °C for 320 min (1:5 Cd:Se ratio). The mean particle diameter is 4.1 nm, in good agreement with the size estimated from the exciton absorption peak (4.3 nm). Figure 6 also presents the HRTEM image of a single CdSe

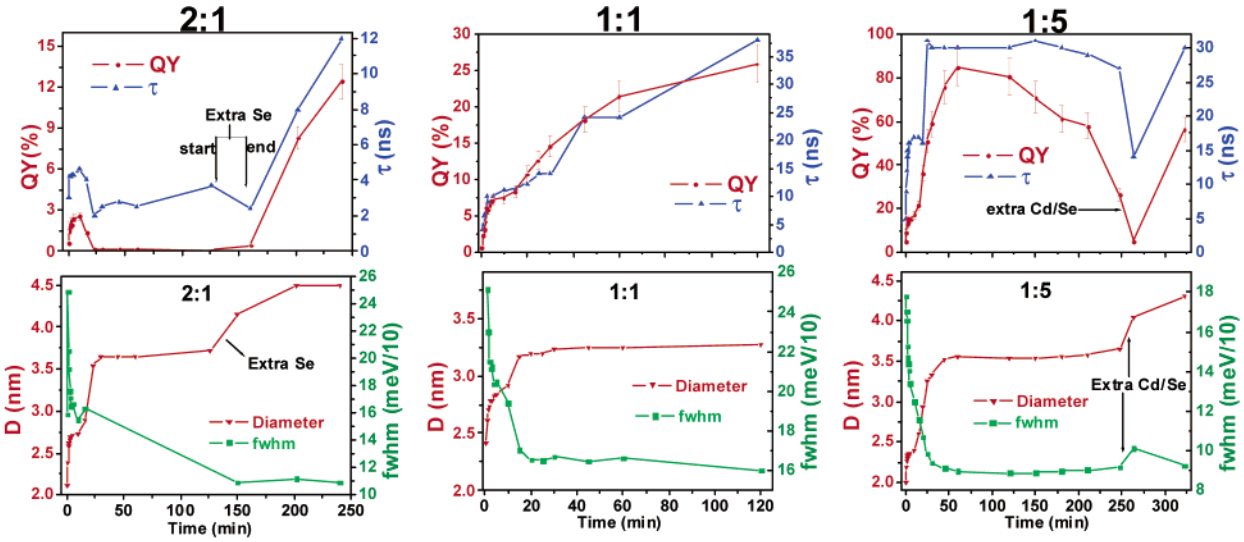

Figure 5. Temporal evolution of the band-edge photoluminescence quantum yields (QY, red circles), lifetimes (τ, blue up triangles), fwhm (green squares), and particle sizes (D, red down triangle) of crude solutions of colloidal CdSe nanocrystals during their growth at 240 °C under three different Cd:Se precursor ratios (2:1, 1:1, and 1:5, from left to right). Trend lines (solid) are added to guide the eyes.

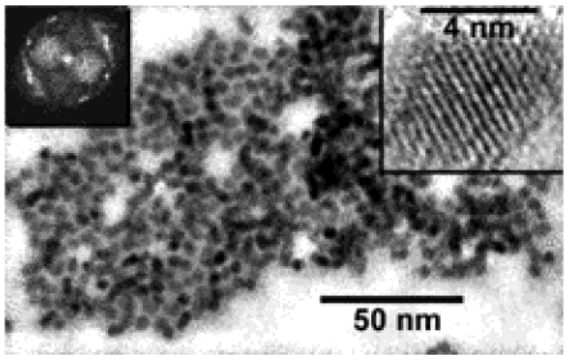

Figure 6. TEM image of a sample of CdSe nanocrystals grown at 240 °C under a 1:5 Cd:Se precursor ratio. The inset at the top right shows a HRTEM image for a single CdSe nanocrystal from the same ensemble. A selected area electron diffraction pattern is presented in the top left inset.

nanocrystal from the same ensemble and a selected area electron diffraction pattern. It can be observed that the nanoparticles are well crystallized, with interplanar distances of 3.3 Å, which is consistent with the (101) planes of wurtzite CdSe (viz. 3.289 Å). The crystal lattice appears to be faultless in all the CdSe nanocrystals investigated.

The lifetime and the QY trends are strongly correlated for all three Cd:Se ratios, even for the initial samples (Figure 5). For the excess of Cd precursor, the QY quickly increases to a few percent and then drops to almost zero, showing that a Cd excess results in very low quantum yields. Addition of an excess of Se monomer revives the CdSe nanocrystals luminescence, increasing the quantum yield to more than 10%. For the 1:1 ratio, both the lifetime and the quantum yield continuously increase in time, although the ensemble growth and focusing stop at ∼30 min after the hot injection. When the lifetime of the band-edge luminescence has achieved its longest value (∼35 ns) and a nearly single-exponential decay, the ensemble quantum yield is still low (25%).

Growth under an excess of Se monomer leads to the most efficient CdSe nanocrystals (quantum yields up to ∼90%). The ensemble quantum yield reaches the maximum value at about the same time as the growth stops and the fwhm reaches its minimum, remains stable for ∼60 min and then starts to decrease. The addition of extra Cd:Se initially brings the QY down to just a few percent, but after 60 min of annealing, it recovers to a high value (60%). It is interesting to notice that the lifetimes for the 1:5 Cd:Se ratio synthesis do not follow exactly the QY trend, but rather, they reach the maximum value faster and do not decrease substantially when the QY starts to drop, except after the addition of extra precursors, when the lifetimes again follow the drop and recovery of the QY.

Discussion

The results presented in the previous section show how very high band-edge PL quantum yields (up to ∼90% at room temperature) can be achieved reproducibly for colloidal CdSe nanocrystals grown in the coordinating solvent 53 wt %TOPO: 26 wt %HDA: 21 wt %TOP, without any postpreparative treatment, when growth is carried out at an ideal temperature (240 °C) and under an excess of Se monomer. As will be discussed below these growth conditions lead to an optimum surface passivation of the nanocrystals.

To illustrate the degree of reproducibility achieved in this work, Figures 3 and 5 show the results for two different syntheses carried out under the same conditions (i.e., 1:5 Cd: Se ratio; [CdSe]= 67 mmol/Kg solvent, growth at 240 °C). It can be clearly seen that the general trends are the same in both cases. However, small differences are observed between the two syntheses with respect to the maximum QY (70 and 85%, respectively), minimum fwhm (140 and 90 meV, respectively), and stabilized nanocrystal diameter (3.3 and 3.5 nm, respectively). These differences probably arise from the hot-injection (e.g., from small variations in the duration of the injection) and from temperature fluctuations (specially during the injection and heating from 150 °C to the growth temperature).

The role of the surface in determining the luminescence quantum yields of semiconductors has long been recognized[3−6,23−25,33,34,50−52] and has been ascribed to the higher concentration of defects at the surface (e.g., unsaturated bonds, ion vacancies, or disorder), which gives rise to a high density of mid-gap states acting as electron and hole traps.[50−52] The surface properties are expected to have a large influence on the optical properties of semiconductor nanocrystals, because of the high surface-to-volume ratio of small particles.[3−6] To understand how the growth conditions determine the surface structure of CdSe nanocrystals, we will first discuss the contribution of each

individual parameter (i.e., growth temperature and Cd:Se ratio) and later consider the effect of their combination. The solvent composition is known to have a large impact on the growth kinetics and on the quantum yields of CdSe nanocrystals.[28,29,33] However, to make the roles of the growth temperature and precursor ratio more evident, the investigations reported in this work were all carried out using the same solvent composition. Therefore, the influence of changing the coordinating solvent will not be addressed.

The influence of the growth temperature can be understood in terms of the growth rates and surface annealing. The initial period after the hot-injection is characterized by rapid growth, which results in surface disorder, and thus low quantum yields. Surface ordering and reconstruction can subsequently take place during annealing, reducing the concentration of defects and increasing the quantum yields. It is observed that 240 °C is the best temperature for this surface reorganization process to occur (Figure 3). Further, the use of such a low growth temperature has also proven to be very advantageous in maintaining high QYs (60−85%) for hours during the growth. In contrast, the high QYs (∼85%) reported by Qu and Peng[33] for growth at 290 °C under a 1:5 Cd:Se ratio were stable for only ∼5 min during the growth.

The lower QYs achieved at $T_{growth} < 240$ °C (e.g., 20% at 170 °C, Figure 3) imply that there is an activation energy for surface ordering and reconstruction. This is clearly demonstrated by the fact that when the temperature is increased from 170 to 240 °C there is a concomitant improvement of the quantum yields, even though the growth rates increase. Higher growth temperatures ($T_{growth} > 240$ °C, Figure 3) lead to faster growth rates and therefore the surface roughening and degradation compete with surface ordering. Higher temperatures induce faster surface degradation (e.g., $t > 25$ min at 280 °C, Figure 3), which reduces the luminescence efficiency shortly after the maximum efficiency has been reached. The surface degradation is also observed at 240 °C but after much longer heating times ($t > 120$ min, Figure 5), as expected for a thermally induced process. Surface degradation can be stopped by quenching the ensemble of CdSe nanocrystals with the optimum surface to room temperature. Furthermore, the slow addition of extra Cd/Se precursors to a solution of CdSe nanocrystals heated for 250 min at 240 °C, and thus with a decreased QY (25%), has the effect of bringing the QY back to a high value (60%), after 60 min annealing (Figure 5, 1:5). This clearly shows that the thermally induced quenching sites are due to a degraded surface, because overgrowth of a fresh surface eliminates them. If the quenching sites responsible for the decrease in the quantum efficiency to 25% were in the "bulk" of the nanocrystal, no recovery of the QY would be expected after growing a fresh surface over the quantum dot. The nature of this surface degradation is still unclear, and it can be related to defect creation at the nanocrystal surface (e.g., ion vacancies) and/or in the passivating shell (e.g., loss of ligands). This experiment also provides additional evidence for the surface model presented above, implying that a fresh CdSe surface is initially disordered (QY decreases immediately after the addition, Figure 5, 1:5) but becomes ordered upon annealing (QY increases 60 min after the addition, Figure 5, 1:5).

An excess of Se monomer is essential to achieve high quantum yields (Figure 5). The enhancement of the QYs after slow addition of extra Se or extra Cd:Se precursors (2:1 and 1:5 synthesis, respectively, Figure 5) clearly demonstrates that the surface is responsible for the nonradiative decay. Therefore, the influence of the excess of Se can be ascribed to changes in the surface structure. Surface annealing under an excess of Se will favor Se-rich facets and therefore reduce the amount of Cd dangling bonds. In addition, Cd−Se nonpolar facets can undergo spontaneous surface reconstruction,[53] and polar Se facets, although requiring activation energy, will be more effectively reconstructed by pair formation than the polar Cd facets.[53] Reconstruction leads to surface auto-compensation (i.e., redistribution of the electronic density in such a way that both Cd and Se dangling bonds are saturated), thus moving the surface state energies away from the band-gap.[53]

The use of an excess of the Se precursor (1:5, Figure 5) leads to the slowest growth and focusing rates and the narrowest size distribution (nearly monodisperse ensembles, fwhm = 90 meV; size dispersion ∼5%). This can be ascribed to a large monomer oversaturation during the growth,[44,45,49] which is achieved because of the much higher solubility of TOP−Se in TOP−TOPO−HDA, in comparison to the Cd monomers. It can be argued that the slower growth rates reduce surface disorder and facilitate surface ordering and reconstruction, thus being advantageous for achieving higher QYs. Further, the excess of Se may also be beneficial because it prevents the formation of metallic cadmium. As shown above (Results section), the injection of $Cd(CH_3)_2$ in hot TOPO−HDA under strictly water and oxygen-free conditions leads to the formation of Cd^0, which may cause the formation of n-doped (and thus nonluminescent) CdSe nanocrystals.

The band-edge PL decay of TOPO capped CdSe (QY = 3%[42]) and CdSe/ZnS (QY ∼ 30−50%[23,25,35]) nanocrystals has been reported to be nonexponential with a lifetime of ∼5−30 ns.[23,25,35,42] In this work, we have observed a wide range of ensemble decay dynamics for the band edge luminescence of TOPO−TOP−HDA capped CdSe nanocrystals, going from strongly nonexponential decays with a 1/e lifetime of ∼4 ns to single exponential decays with a lifetime of ∼30 ns (Figures 3−5). The clear correlation observed between the trends for the lifetimes and for the quantum yields implies that the exciton radiative lifetime (τ_{RAD}) is essentially constant throughout the growth process of the CdSe nanocrystals, whereas the rate of the competing nonradiative decay process (A_{NRAD}) varies, depending on the surface structure ($QY = A_{RAD}/(A_{RAD} + A_{NRAD})$; where $A_{RAD} = \tau_{RAD}^{-1}$). The decay of the high QY (≥60%) samples is dominated by the radiative exciton emission rate ($\approx 3 \times 10^7\ s^{-1}$). The analysis of the band-edge luminescence decay is complicated for the lower quantum yield samples, because in this case the decays are characterized by a complex distribution of shorter lifetimes, depending on the nonradiative processes dominating for different particles within the ensemble of crystallites. In addition, the decay curves of samples with quantum yields below ∼20% often presented a longer decay tail in the ∼100 ns range, which can be ascribed to a defect-related luminescence.[23]

It is interesting to notice that the correlation between the QY and the lifetimes is not always present. A good example of such a behavior is observed in the beginning of the surface degradation for the 1:5 Cd:Se ratio samples grown at 240 °C (Figure 5, 1:5 synthesis), where the QY decreases without a substantial change in the lifetime. This indicates that the surface degradation quenches the luminescence of a fraction of the ensemble, whereas the unaffected particles remain fully efficient. Because the decay measurements are biased toward the "bright" particles, the lifetimes will reflect the decay dynamics of the efficient CdSe nanocrystals. The lifetimes start to change only when the QY reaches low values (≤30%). In this case, most photons will be emitted by the inefficient particles, which then compose the

majority of the ensemble, and the kinetics of trapping/detrapping will be reflected in the luminescence decay.

Conclusions

The key roles of both the growth temperature and the cadmium to selenium precursor ratio in determining the size polydispersity, band-edge photoluminescence quantum yields, and exciton lifetimes of colloidal CdSe nanocrystals have been extensively investigated employing a one-pot synthesis in TOPO:HDA:TOP as the coordinating solvent. It has been demonstrated that by a judicious choice of the Cd:Se ratio (1:5) and the growth temperature (240 °C) highly luminescent nearly monodisperse CdSe nanocrystals may be reproducibly obtained, without any postpreparative treatment. Among the advantages of employing these growth conditions are high (up to ~90%) and reproducible ensemble band-edge PL quantum yields, relatively long time period (60−120 min) during the growth over which the quantum yields are at a maximum, no defocusing of the narrow particle size distributions, and access to a range of particle sizes (3−8 nm) through furnishing of additional precursor solution. The results show that the surface of colloidal CdSe nanocrystals is initially disordered and undergoes ordering and reconstruction upon annealing. The above-mentioned growth conditions favor surface ordering and reconstruction, thus leading to an optimum surface, which is defect-free and well passivated.

Acknowledgment. This work was financially supported by the Council for Chemical Sciences of The Netherlands Organization for Scientific Research (CW-NWO) and the Breedtestrategie program of the University of Utrecht. The authors are grateful to Dr. Hans Meeldijk (EMSA, Debye Institute, Universiteit Utrecht, The Netherlands) for TEM and HRTEM measurements.

References and Notes

(1) Gaponenko, S. V. *Optical Properties of Semiconductor Nanocrystals*; Cambridge University Press: Cambridge, U.K., 1998.
(2) Brus, L. *Appl. Phys. A* **1991**, *53*, 465.
(3) Alivisatos, A. P. *J. Phys. Chem.* **1996**, *100*, 13226.
(4) Wang, Y.; Herron, N. *J. Phys. Chem.* **1991**, *95*, 525.
(5) Weller, H. *Angew. Chem., Int. Ed. Engl.* **1993**, *32*, 41.
(6) Henglein, A. *Chem. Rev.* **1989**, *89*, 1861.
(7) Colvin, V. L.; Schlamp, M. C.; Alivisatos, A. P. *Nature* **1994**, *370*, 354.
(8) Sundar, V. C.; Lee, J.; Heine, J. R.; Bawendi, M. G.; Jensen, K. F. *Adv. Mater.* **2000**, *12*, 1102.
(9) Gao, M.; Lesser, C.; Kirstein, S.; Mohwald, H.; Rogach, A. L.; Weller, H. *J. Appl. Phys.* **2000**, *87*, 2297.
(10) Tessler, N.; Medvedev, V.; Kazes, M.; Kan, S. H.; Banin, U. *Science* **2002**, *295*, 1506.
(11) Klimov, V. I.; Mikhailovsky, A. A.; Xu, S.; Hollingsworth, J. A.; Leatherdale, C. A.; Eisler, H. J.; Bawendi, M. G. *Science* **2000**, *290*, 314.
(12) Kazes, M.; Lewis, D. Y.; Ebenstein, Y.; Mokari, T.; Banin, U. *Adv. Mater.* **2002**, *14*, 317.
(13) Qi, J.; Masumoto, Y. *Solid State Commun.* **1996**, *99*, 467.
(14) Vlasov, Y. A.; Yao, N.; Norris, D. J. *Adv. Mater.* **1999**, *11*, 165.
(15) Bruchez, M., Jr.; Moronne, M.; Gin, P.; Weiss, S.; Alivisatos, A. P. *Science* **1998**, *281*, 2013.
(16) Shan, W. C. W.; Nie, S. *Science* **1998**, *281*, 2016.
(17) Han, M.; Gao, X.; Su, J. Z.; Nie, S. O. *Nat. Biotechnol.* **2001**, *19*, 631.
(18) Gerion, D.; Pinaud, F.; Williams, S. C.; Parak, W. J.; Zanchet, D.; Weiss, S.; Alivisatos, A. P. *J. Phys. Chem. B* **2001**, *105*, 8861.
(19) Mattoussi, H.; Mauro, J. M.; Goldman, E. R.; Green, T. M.; Anderson, G. P.; Sundar, V. C.; Bawendi, M. G. *Phys. Stat. Sol. (B)* **2001**, *224*, 277.
(20) Tran, P. T.; Goldman, E. R.; Anderson, G. P.; Mauro, J. M.; Mattoussi, H. *Phys. Stat. Sol. (B)* **2002**, *229*, 427.
(21) Murray, C. B.; Norris, D. J.; Bawendi, M. G. *J. Am. Chem. Soc.* **1993**, *115*, 8706.
(22) Katari, J. E. B.; Colvin, V. L.; Alivisatos, A. P. *J. Phys. Chem.* **1994**, *98*, 4109.
(23) Hines, M. A.; Guyot-Sionnest, P. *J. Phys. Chem.* **1996**, *100*, 468.
(24) Peng, X.; Schlamp, M. C.; Kadavanich, A. V.; Alivisatos, A. P. *J. Am. Chem. Soc.* **1997**, *119*, 7019.
(25) Dabbousi, B. O.; Rodriguez-Viejo, J.; Mikulec, F. V.; Heine, J. R.; Mattoussi, H.; Ober, R.; Jensen, K. F.; Bawendi, M. G. *J. Phys. Chem. B* **1997**, *101*, 9463.
(26) Peng, X.; Manna, L.; Yang, W.; Wickham, J.; Scher, E. C.; Kadavanich, A.; Alivisatos, A. P. *Nature* **2000**, *404*, 59.
(27) Jacobsohn, M.; Banin, U. *J. Phys. Chem. B* **2000**, *104*, 1.
(28) Qu, L.; Peng, Z. A.; Peng, X. *Nano Lett.* **2001**, *1*, 333.
(29) Talapin, D. V.; Rogach, A. L.; Kornowski, A.; Haase, M.; Weller, H. *Nano Lett.* **2001**, *1*, 207.
(30) Peng, Z. A.; Peng, X. *J. Am. Chem. Soc.* **2001**, *123*, 1389.
(31) Cumberland, S. L.; Hanif, K. M.; Javier, A.; Khitrov, G. A.; Strouse, G. F.; Woessner, S. M.; Yun, C. S. *Chem. Mater.* **2002**, *14*, 1576.
(32) Peng, Z. A.; Peng, X. *J. Am. Chem. Soc.* **2002**, *124*, 3343.
(33) Qu, L.; Peng, X. *J. Am. Chem. Soc.* **2002**, *124*, 2049.
(34) Talapin, D. V.; Rogach, A. L.; Shevchenko, E. V.; Kornowski, A.; Haase, M.; Weller, H. *J. Am. Chem. Soc.* **2002**, *124*, 5782.
(35) Ebenstein, Y.; Mokari, T.; Banin, U. *Appl. Phys. Lett.* **2002**, *80*, 4033.
(36) Van Sark, W. G. J. H. M.; Frederix, P. L. T. M.; Van den Heuvel, D. J.; Gerritsen, H. C.; Bol, A. A.; van Lingen, J. N. J.; de Mello Donegá, C.; Meijerink, A. *J. Phys. Chem. B* **2001**, *105*, 8281.
(37) Kuno, M.; Lee, J. K.; Dabbousi, B. O.; Mikulec, F. V.; Bawendi, M. G. *J. Chem. Phys.* **1997**, *106*, 9869.
(38) Klimov, V. I.; McBranch, D. W.; Leatherdale, C. A.; Bawendi, M. G. *Phys Rev. B* **1999**, *60*, 13740.
(39) Bawendi, M. G.; Carroll, P. J.; Wilson, W. L.; Brus, L. E. *J. Chem. Phys.* **1992**, *96*, 946.
(40) Nirmal, M.; Norris, D. J.; Kuno, M.; Bawendi, M. G. *Phys Rev. Lett.* **1995**, *75*, 3728.
(41) Underwood, D. F.; Kippeny, T.; Rosenthal, S. J. *J. Phys. Chem. B* **2001**, *105*, 436.
(42) Burda, C.; Link, S.; Mohamed, M.; El-Sayed, M. *J. Phys. Chem. B* **2001**, *105*, 12286.
(43) Van Leeuwen, P. W. N. M.; Groeneveld, W. L. *Inorg. Nucl. Chem. Lett.* **1967**, *3*, 145.
(44) Peng, X.; Wickham, J.; Alivisatos, A. P. *J. Am. Chem. Soc.* **1998**, *120*, 5343.
(45) Talapin, D. V.; Rogach, A. L.; Haase, M.; Weller, H. *J. Phys. Chem. B* **2001**, *105*, 12278.
(46) Bol, A. A.; Meijerink, A. *J. Phys. Chem. B* **2001**, *105*, 10203.
(47) Van Dijken, A.; Janssen, A. H.; Smitsmans, M. H. P.; Vanmaekelbergh, D.; Meijerink, A. *Chem. Mater.* **1998**, *10*, 3513.
(48) Kapitonov, A. M.; Stupak, A. P.; Gaponenko, S. V.; Petrov, E. P.; Rogach, A. L.; Eychmuller, A. *J. Phys. Chem. B* **1999**, *103*, 10109.
(49) Peng, Z. A.; Peng, X. *J. Am. Chem. Soc.* **2001**, *123*, 183.
(50) Euteneuer, A.; Hellmann, R.; Gobel, E.; Shevel, S.; Vozny, V.; Vytrykhivsky, M.; Petri, W.; Klingshirn, C. *J. Crystal Growth* **1998**, *184/185*, 1081.
(51) Shimakawa, K.; Kolobov, A.; Elliot, S. R. *Adv. Phys.* **1995**, *44*, 475.
(52) Kepler, K. D.; Lisensky, G. C.; Patel, M.; Sigworth, L. A.; Ellis, A. B. *J. Phys. Chem.* **1995**, *99*, 16011.
(53) Kahn, A. *Surface Science* **1994**, *299/300*, 469.